JOURNAL OF MATERIALS SCIENCE 25 (1990) 3990–4000

The structure and properties of oriented chain-extended polyethylenes

A. K. POWELL, G. CRAGGS, I. M. WARD
Department of Physics, University of Leeds, Leeds LS2 9JT, UK

Highly oriented polyethylene can be produced by a route which involves firstly annealing the material at a pressure of 450 MPa and a temperature 234° C so that ideally it enters the intermediate phase and chain extended material is produced. This is followed by hydrostatic extrusion of the material to align the molecular chains.

The apparatus and procedure for processing the material by this route is described. The products produced both before and after hydrostatic extrusion have been structurally analysed and the density, orientation and DSC characteristics of two polyethylene materials are presented. The mechanical behaviour of the extrudates has been determined, particularly in terms of their dynamic bending modulus (E) and shear modulus (G). To aid understanding, an aggregate model has been developed which shows a linear relationship between $1/E$ and $1/G$. The dynamic experimental results show good agreement with this model and the structural data adds further support to the findings.

1. Introduction

In a previous publication from our laboratory a study was reported where polyethylene was annealed at high temperature under pressure to produce chain extended material, and this was subsequently hydrostatically extruded to produce an oriented product [1]. It was of particular interest that a product of considerably enhanced stiffness was obtained for a comparatively modest extrusion ratio, although the relationship between crystal length and long period was apparently similar to that for oriented polyethylene produced by hydrostatic extrusion of bulk polymer crystallized at atmospheric pressure.

A recent paper by Chuah and Porter [2] describes how polyethylene annealed under pressure was extruded at 100° C through a conical die in the Instron capillary rheometer. It was concluded that highly chain-extended material draws poorly. The material had lamellar thicknesses comparable to the molecular chain length and was found to contain few trapped entanglements and interlamellar links to provide continuity and stress transfer for effective orientation during drawing.

The evident contradiction between the results of Chuah and Porter and those reported from this laboratory have led us to re-examine very much more carefully the hydrostatic extrusion of pressure-annealed polyethylene. It will be shown that under appropriate conditions it is feasible to obtain very highly oriented chain-extended polyethylene with very high axial stiffnesses for comparatively modest extrusion ratios (~ 10).

2. Experimental procedure

2.1. Introduction

It has previously been shown that highly oriented polymers may be produced by hydrostatic extrusion using billets which have been produced either by melt crystallization or alternatively have been pressure crystallized and are in chain extended form. In an early study by Sahari, Parsons and Ward [1], various routes for producing oriented polyethylene were investigated including the hydrostatic extrusion of polyethylene at temperatures above 230° C and pressures greater than 400 MPa where the material was in the intermediate phase as identified by Bassett and coworkers [3, 4] while being extruded. The results of this work indicated that the route involving the initial production of chain extended billets followed by a separate stage where the billets were hydrostatically extruded, had potential and was worthy of further investigation. This paper describes the further work that has been carried out into this processing route.

2.2. High pressure annealing facility

A high pressure annealing facility was specifically designed and developed so as to be capable of pressure annealing cylindrical billets of polyethylene up to 8 mm diameter and 240 mm long at pressures up to 600 MPa and temperatures of 250° C. In the experimental programme it was not expected to exceed pressures to 500 MPa and temperatures of 240° C. The facility, shown in Fig. 1, consists essentially of two cylinders which have threaded connections so that they can be screwed together. The upper cylinder supports and guides the piston while the lower cylinder containing the polyethylene billet immersed in silicone fluid Dow Corning (DC 550) was capable of withstanding the above design pressure. Both cylinders were shrouded in heater bands which together with appropriate lagging at the cylinder ends, enabled

0022–2461/90 $03.00 + .12

the temperature distribution in the zone containing the billet to be held constant to within $\pm 0.5°$ C. The whole apparatus was mounted in the compression region of a 500 kN screw driven universal testing machine and this enabled the rate of displacement of the piston to be accurately controlled.

The high annealing pressures and temperatures presented severe conditions for the seals between the piston and cylinder. A Vitron '0' ring – mitre ring combination was eventually found to be satisfactory with the piston well supported in the upper cylinder. Particular attention was given to the measurement of billet temperature. The temperature of a polyethylene billet when in its pressure annealing position could not be measured directly without drilling radial holes along its length and thereby making it of little further use. Billet temperature was found to be equal to that measured by thermocouples along the cylinder centre line with no billet present but with the silicone fluid pressurized to 450 MPa. A steady state temperature distribution was established along the entire length of the pressure vessel with the temperature deviation being no more than $\pm 0.5°$ C from a set value, usually 234° C.

Fluid pressure was measured using a pressure transducer which consisted of strain gauges attached to a length of high pressure tubing which was connected as a branch pipe to the high pressure cylinder via the end closure. Calibration of the transducer showed that pressure could be reliably measured to within ± 1 MPa. In early tests freezing of the silicon fluid occurred in the cool high pressure tubing at a pressure of 300 MPa, thereby limiting its ability to measure pressure. Raising the tube temperature to 150° C using heating tapes and calibrating the transducer under these environmental conditions enabled repeatable pressure measurement to be made to within the above limits.

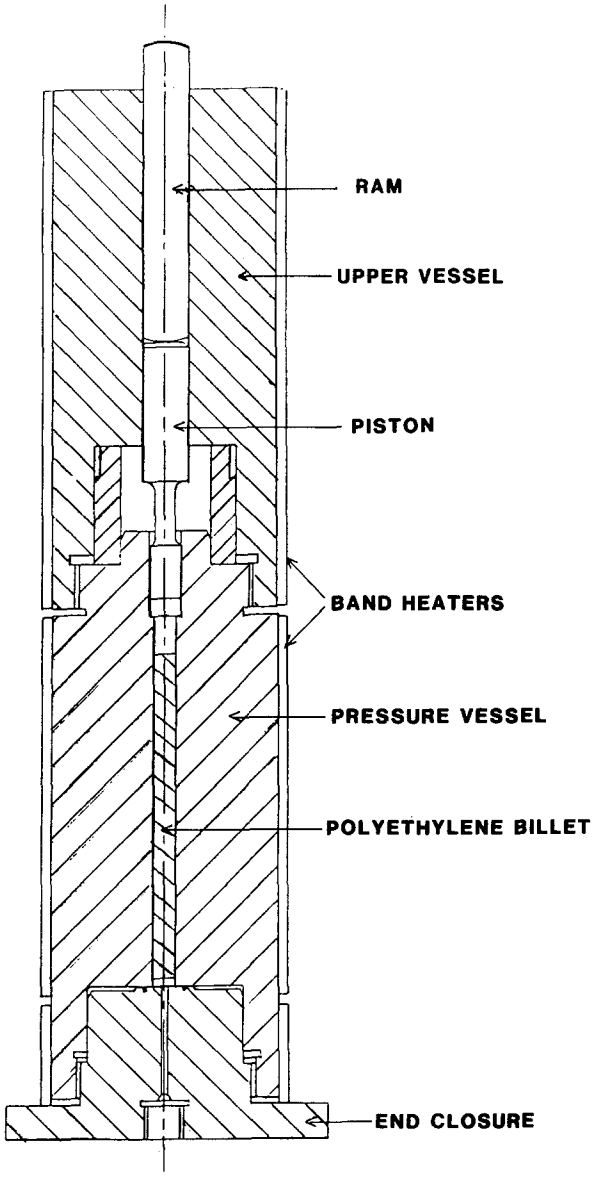

Figure 1 Schematic diagram of pressure annealing test apparatus. The entire system is seated on a support stand to enable the thermocouple assembly and the pressure transducer to be connected via the end enclosure.

2.3. Pressure annealing procedure

To pressure anneal in the intermediate phase, the pressure and temperature of a billet must reach values which when plotted on Fig. 2 lie in the intermediate phase zone as defined by Bassett and Carder [3]. The higher the annealing pressure the greater the temperature band of the hexagonal phase. Many experiments were carried out at 450 MPa pressure and 234° C where the band was typically 4° C. The pressure–temperature path followed by the material before entering the hexagonal phase, is not thought to influence the final product properties and in the pressure annealing experiments the procedure followed produced path OABCDEF which is shown in Fig. 2 and described below.

With the billet located in the pressurizing chamber in silicon fluid, the pressure in the vessel was raised to 300 MPa by applying load to the piston, so reaching point A. The heater band around each cylinder was then energized and with the piston locked in position the temperature and pressure were allowed to rise until the desired pressure of 450 MPa (point B) was reached. The temperature reached at this stage was approximately 150° C and this step took about 15 min.

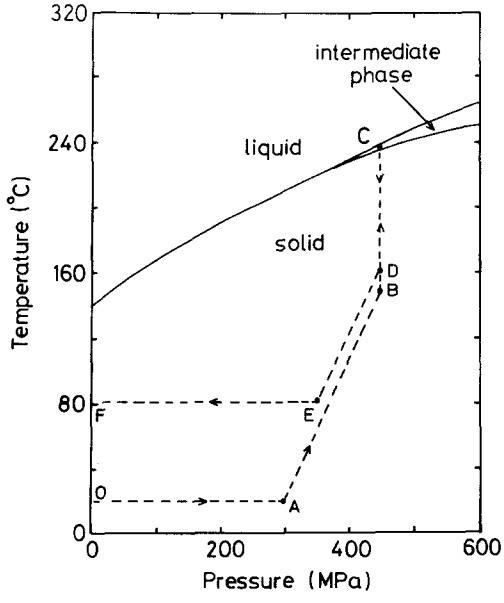

Figure 2 Temperature–pressure phase diagram for polyethylene showing pressure annealing path.

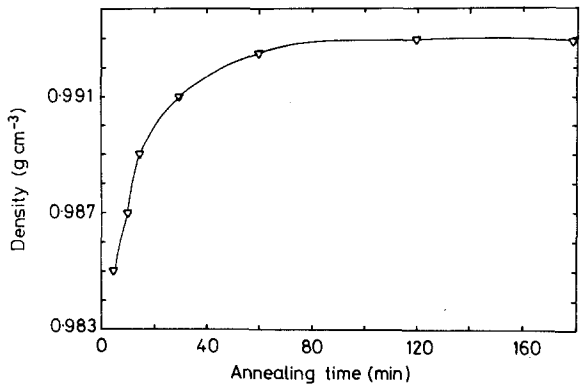

Figure 3 Variation of the density of R006-60 billets after pressure annealing in the intermediate phase for different annealing times. (Annealing temperature 234° C, pressure 450 MPa).

From this point temperature was allowed to rise slowly at constant pressure by appropriately withdrawing the piston in the cylinder until the temperature was within 5° C of the desired annealing temperature. Thereafter, temperature was increased at about 0.5° C min^{-1} until the final annealing temperature was reached (point C). The polyethylene billet was then annealed for the desired length of time.

The cooling procedure was designed to prevent the billet from ever reaching melt conditions and consisted of first switching off the heaters and allowing the cylinders to cool under a forced air cooling system with the pressure held constant by appropriate displacement of the piston. The billet cooled to about 160° C in 30 min with this arrangement (point D) and thereafter pressure was allowed to decrease with temperature under constant volume conditions. When below 80°C, the residual pressure was released and the billet cooled naturally to ambient temperature following path EFO.

2.4. Hydrostatic extrusion

The billets after pressure annealing were hydrostatically extruded in a castor oil environment using a Fielding Platt hydrostatic system capable of generating pressures up to 700 MPa. Contrary to expectation they were found to be ductile after annealing and were extruded without difficulty to the desired extrusion ratio. All hydrostatic extrusions were carried out at 100° C with fluid pressure being initially increased to a value which produced a short length of extrudate. Thereafter, a haul off load was applied to the extrudate to keep it straight and pressure was adjusted to produce a constant extrudate speed during the remaining part of the extrusion.

3. Results

3.1. Characterization of pressure-annealed polyethylenes prior to hydrostatic extrusion

The pressure–annealed samples were characterized by density, enthalpy of fusion and melting point. The key results for BP Chemicals grade R006-60 annealed at 234° C and 450 MPa are summarized in Table I and Figs 3 and 4.

It can be seen from Table I and Fig. 3 that for the above annealing conditions the density rises very rapidly with increasing annealing time up to about 60 min, after which there is a much lower rate of increase, and indeed no significant difference between 120 and 180 min. The peak melting point, on the other hand reaches a value of 139.65° C after 5 min annealing, suggesting that even at short times there is an appreciable amount of chain-extended material produced.

The results for the H020-54P grade are also given in Table I, where a standard annealing time of 60 min was chosen. It can be seen that there appears to be a small gradual increase in density with increasing annealing temperature, and close inspection of the results for the R006-60 grade confirm that this effect can be seen for this material also.

TABLE I Summary of the initial chain-extended material density for medium to high molecular weight polyethylene

Annealing Conditions				Characteristics		
Material	Temperature (° C)	Time (min)	Pressure (MPa)	Density (g cm^{-3})	Crystallinity (%)	Melting point (° C)
R006-60	234	5	450	0.9850	92.8	
(M_w = 135000)	234	10	450	0.9870	93.9	139.65
(M_n = 25500)	234	15	450	0.9890	95.2	139.65
	234	30	450	0.9910	96.3	139.65
	234	60	450	0.9925	97.3	139.65
	234	120	450	0.9930	97.6	140.65
	234	180	450	0.9930	97.6	
	236	60	450	0.9930	97.6	140.20
	237	60	450	0.9935	97.9	
	239	60	450	0.9942	98.4	
	234	60	475	0.9910	96.4	139.00
	234	60	500	0.9860	93.4	
H020-54P	234	60	450	0.9855	93.0	139.50
(M_w = 312000)	237	60	450	0.9880	94.6	141.00
(M_n = 13600)	239	60	450	0.9905	96.1	142.00
High pressure isothermally melt crystallized R006-60	236	60	450	0.9937	98.0	140.00

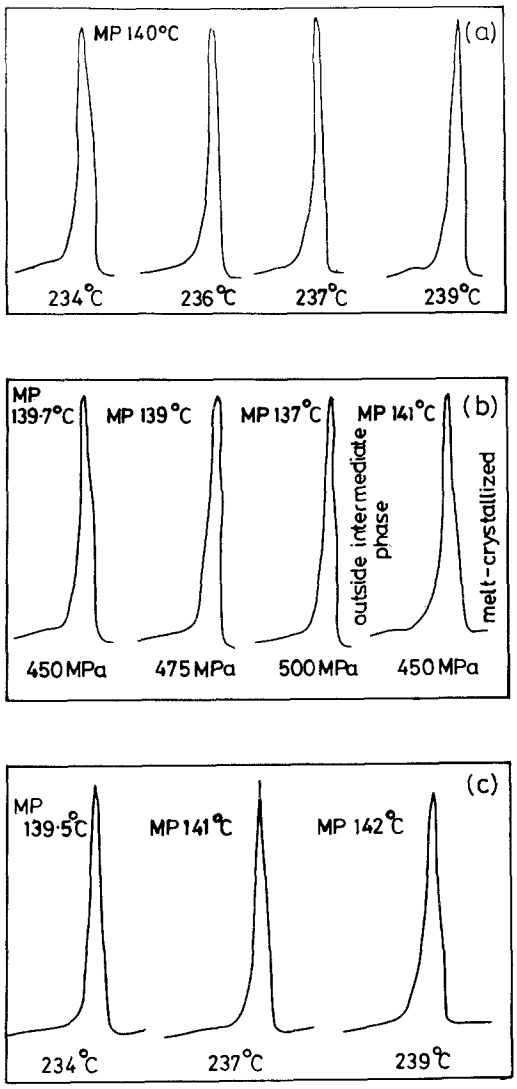

Figure 4 Endotherms of pressure annealed samples. (a) R006-60 billets pressure annealed at 450 MPa for 1 h at temperature shown. (b) R006-60 billets pressure annealed at 234° C for 1 h at pressure shown together with an isothermally melt crystallized sample. (c) H020-54P billets pressure annealed at 450 MPa at temperature shown.

Table I also shows results for R006-60 grade isothermally crystallized at high pressures from the melt, as distinct from the pressure annealing treatment uniformly adopted for all the other samples. The density and melting point are similar to those of the pressure annealed samples, in spite of the known differences in gross morphology.

The DSC results for the R006-60 and H020-54P grades are shown in Fig. 4, and in general two or three overlapping endotherms can be observed. In all cases the highest peak melting point occurs at approximately 140° C, corresponding to the melting of large chain-extended lamellae. A much smaller endotherm can be seen at a lower temperature, and following previous research, this is attributed to the melting of low molecular weight fractions which segregate during the annealing treatment and recrystallize as chain-folded lamellae. From Fig. 4a it can be seen that the low temperature endotherm becomes progressively more intense with increasing annealing temperature until it reaches a constant value when annealing occurs in the intermediate phase. This behaviour is consistent with earlier studies by previous workers [3]. It can be seen from Fig. 4a that an endothermic shoulder appears on the low temperature side of the main melting peak, which becomes progressively more intense with increasing annealing temperature. This has been attributed by Bassett and coworkers [3] to crystals of poorer quality formed on cooling from the hexagonal phase. Fig. 4b shows the sensitivity of the annealing treatment to the exact conditions of temperature and pressure. Increasing the pressure to 500 MPa at the annealing temperature of 234° C takes the annealing conditions just outside the regime where the hexagonal phase is formed, so that chain extended material is not produced, and the melting point of the product falls to 137° C. Fig. 4b also shows the result of isothermal crystallization from the melt under pressure at temperatures and pressures within the intermediate phase. The high melting point of 141° C confirms that a chain-extended product has been obtained.

Finally, Fig. 4c shows the melting behaviour of the H020-54P samples. There is again a high melting peak corresponding to the melting of chain-extended material, and a low melting point shoulder which corresponds to the formation of less perfect crystallization at higher annealing temperatures, as observed for the R006-60 samples. In addition there is a small low temperature endotherm corresponding to the chain folded material which segregates during the crystallization process.

3.2. Characterization of the hydrostatically extruded materials

When chain extended R006-60 and H020-54P is hydrostatically extruded to various draw ratios, the melting behaviour of the extrudates is as shown in Fig. 5. The peak melting point remains virtually unchanged, varying by less than 2° C for extrusion ratios up to 10 : 1.

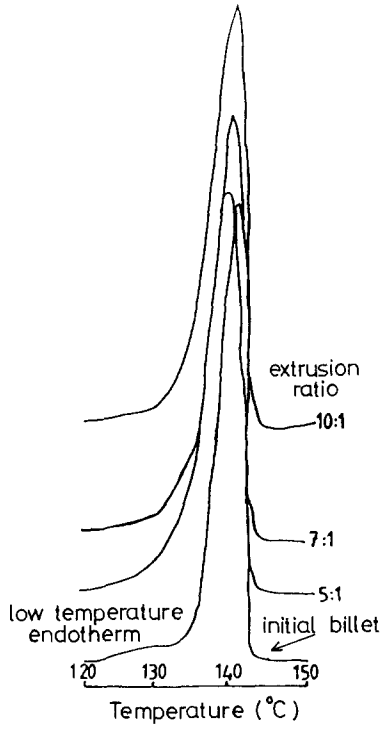

Figure 5 Endotherms of pressure annealed R006-60 and H020-54P after extrusion at the ratio shown.

The lower temperature endotherms, associated with segregated material, decreases in magnitude and merge into the main melting peak by an extrusion ratio of 5 : 1. The slight decrease in peak melting point suggests that there is a certain amount of disruption of the chain-extended material during extrusion. The retention of a high melting point does however suggest that the disruption is not very extensive and that a substantial proportion of the chain extended lamellae survive the imposed deformation. This conclusion is consistent with earlier observations by Bassett *et al.*, [3] and by Chuah and Porter [2].

3.3. Small angle and wide angle X-ray diffraction

The pressure annealed materials did not show a SAXS pattern from which it has been inferred that the long period is in excess of the resolution available with the SERLE small angle camera facility at Leeds University (i.e. greater than about 50 nm). The hydrostatically extruded products, on the other hand, showed a weak two-point pattern similar to that observed by Chuah and Porter [2]. We concur with them that this weak intensity pattern can be attributed to the small fraction of low molecular weight material segregated during the pressure crystallization process.

It is therefore concluded that the majority of the polymer in both the isotropic and oriented samples examined is in chain-extended form. This was confirmed by examination of the breadth of the (0 0 2) reflection using wide-angle X-ray diffractometry. The line profile broadening was of the same order as that exhibited by the copper standard, implying crystal lengths in excess of 100 nm.

3.4. Quantitative measurements of crystalline orientation

Values of orientation functions $\langle P_2(\cos\theta_c)\rangle$ and $\langle P_4(\cos\theta_c)\rangle$ for the various extrudates are collated in Table II and shown in terms of comparisons for different groups of specimens in Fig. 6. The figure shows the four materials listed below, three of which have been subjected to crystallization under high pressures: (i) High pressure-annealed R006-60, (ii) High pressure-annealed H020-54P, (iii) High pressure isothermally crystallized R006-60, (iv) Conventional melt crystallized R006-60. In Fig. 6 the experimental data are compared with the theoretically calculated curves for $P_2(\cos\theta)$ and $P_4(\cos\theta)$ based on the pseudo-affine deformation scheme. It can be seen that the experimental results correspond quite closely with this theoretical scheme, suggesting that the orientation proceeds by reorientation of the chain extended crystals, like an aggregate of rods. This is consistent with the view that there is no breakdown of the chain-extended material, as indicated by the maintenance of a high melting temperature. It is important, however, to note that the alignment of the crystallographic *c* axes, rather than say the *b* axes, does imply the existence of an overall molecular network.

The present results can be clearly distinguished from previous results obtained by Chuah and Porter [2], shown in Fig. 7. In Fig. 7 it can be seen that only material pressure crystallized at 198° C (i.e. outside

TABLE II Summary of the orientation functions obtained from the extrudates of initially chain extended materials

Grade	Annealing condition			R_n	$\langle P_2(\cos\theta_c)\rangle$	$\langle P_4(\cos\theta_c)\rangle$
	Temperature (° C)	Time (min)	Pressure (MPa)			
R006-60	234	5	450	5 : 1	0.8877	0.6645
				7 : 1	0.9196	0.7569
				10 : 1	0.9468	0.8343
	234	15	450	2 : 1	0.4079	−0.1151
				5 : 1	0.8572	0.5878
				7 : 1	0.9281	0.7779
				10 : 1	0.9465	0.8327
	234	60	450	5 : 1	0.8625	0.6061
				8 : 1	0.9236	0.7659
				10 : 1	0.9467	0.8330
	234	120	450	5 : 1	0.8843	0.6580
				7 : 1	0.9274	0.7762
				10 : 1	0.9398	0.8140
	234	180	450	10 : 1	0.9452	0.8303
	237	60	450	10 : 1	0.9460	0.8305
R006-60*	236	60	450	5 : 1	0.8302	0.5275
				7 : 1	0.8687	0.6213
				10 : 1	0.9031	0.7109
H020-54P	234	60	450	5 : 1	0.9062	0.7172
				7 : 1	0.9314	0.7898
				10 : 1	0.9567	0.8628
	237	60	450	5 : 1	0.9265	0.7754
				7 : 1	0.9484	0.8387
				10 : 1	0.9637	0.8849

*High pressure isothermally melt crystallized.

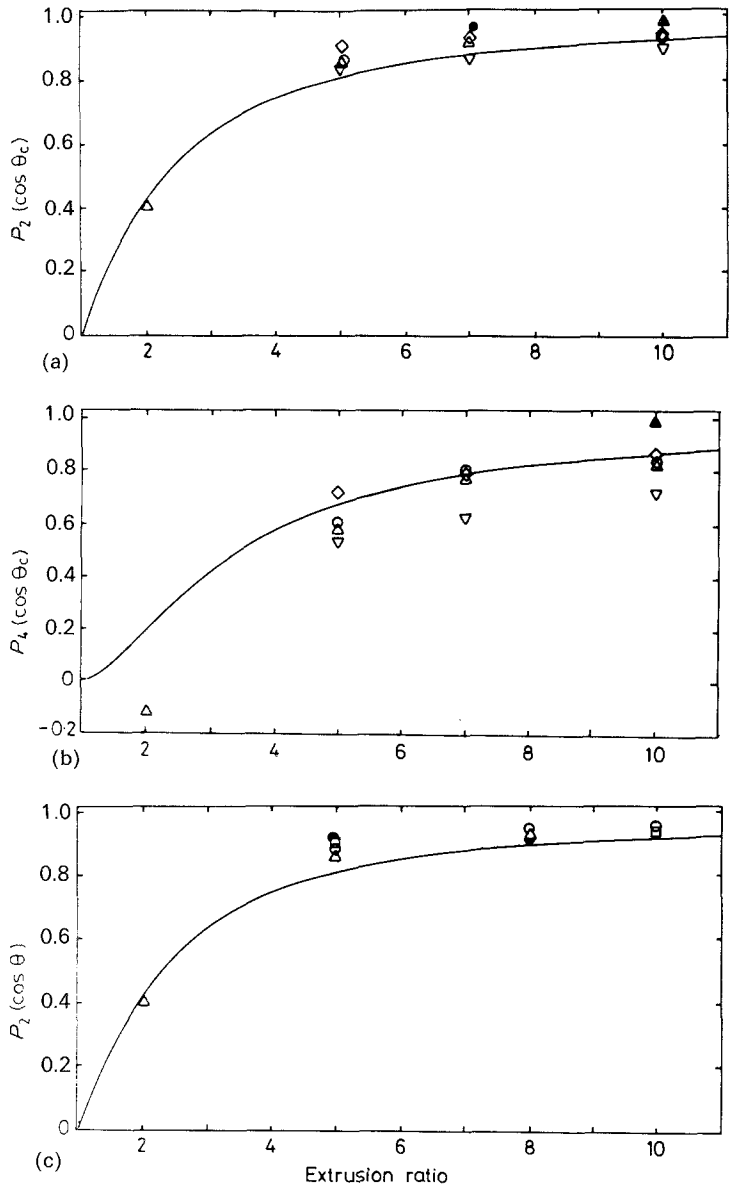

Figure 6 Relationship between orientation function and extrusion ratio for various extrudates. (a) $\langle P_2(\cos\theta_c)\rangle$ relationship with extrusion ratio. (b) $\langle P_4(\cos\theta_c)\rangle$ relationship with extrusion ratio. (c) The effect of annealing time on the $\langle P_2(\cos\theta_c)\rangle$ relationship with extrusion ratio for R006-60. (– pseudo affine, ● R0060-60, 234° C, 5 mins, 450 MPa, △ R006-60, 234° C, 15 mins, 450 MPa, ○ R006-60, 234° C, 60 mins, 450 MPa, ◇ H020-54P, 234° C, 60 mins, 450 MPa, ▽ R006-60, 236° C, 60 mins, 450 MPa, □ R006-60, 234° C, 120 mins, 450 MPa, ▲ Conventional melt-crystallized polythene.)

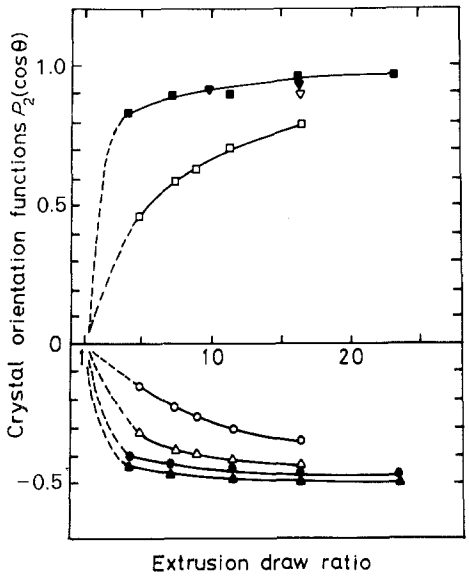

Figure 7 Change of crystal orientation function f for the three crystallographic axes a, b and c for drawn billets 1 (T_c = 221° C) (△, ○, □) and 4 (T_c = 198° C) (▲, ●, ■); f_c of billets 2 (T_c = 216° C) (▽) and 3 (T_c = 207° C) (▼) drawn to EDR 16.4 are inserted for comparison. (From Chuah and Porter [2].)

the regime for chain extension) shows rapid development of orientation with extrusion draw ratio. The material crystallized at 220° C, which will probably also be chain-extended shows much slower development of orientation. On the basis of these results Chuah and Porter concluded that highly chain-extended polyethylene draws poorly. The present results apparently contradict this conclusion. It seems possible that Chuah and Porter's choice of a low molecular weight polymer (M_w = 59 000) led to their result, and that they correctly concluded that their material after pressure annealing had too few chain entanglements. In the present case, the use of much higher molecular weight polymer enables us to achieve a very satisfactory degree of chain extension but to also retain an adequate molecular network, so that the extrusion process is effective in producing molecular orientation.

The development of orientation as a function of the pressure-annealing treatment is shown in Fig. 6c for the R006-60 polymer. It appears that the development of orientation with extrusion ratio is independent of the exact annealing conditions in the intermediate hexagonal phase. Detailed examination of the diffraction

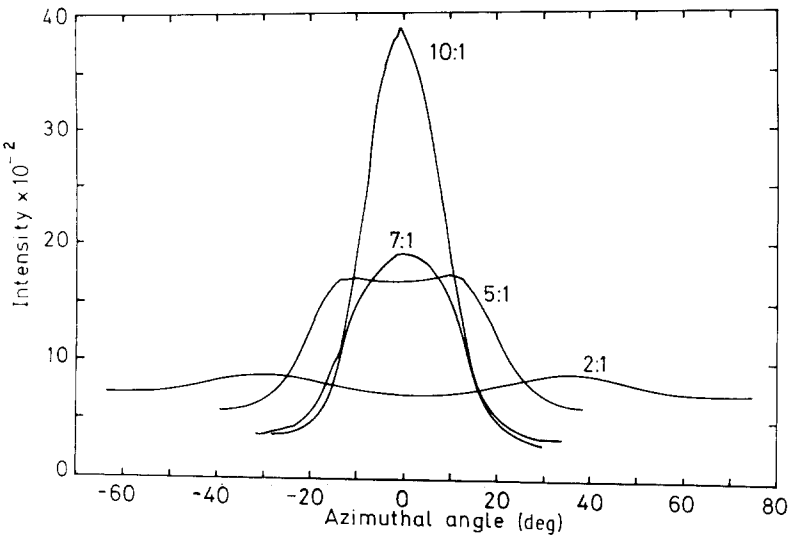

Figure 8 Orientation of R006-60 after pressure annealing at 234° C for 1 h at 450 MPa pressure followed by extrusion at the ratio indicated.

patterns of extruded samples revealed that the development of orientation was, however, not as straightforward as this figure might imply. As shown in Fig. 8, in the earlier stages of the extrusion process, intensification of the (0 0 2) reflections at an angle of about 35° to the draw direction was observed in R006-60. This is similar to development of orientation observed for cold drawn bulk low density polyethylene sheet, and has been attributed to the importance of slip processes in deformation, the maximum shear stress being on planes at 45° to the draw direction.

It is interesting to compare in Fig. 6a, the $\langle P_2(\cos\theta_c)\rangle$ values for the R006-60 and H020-54P polymers when both have been pressure annealed at 234° C and 450 MPa pressure for 60 min and subsequently extruded. Although the values of $\langle P_2(\cos\theta_c)\rangle$ do not differ greatly between the two polymers, careful inspection of the results shows that the values of $\langle \sin^2\theta_c\rangle$ are significantly smaller for the H020-54P polymer. It is suggested that this may be attributed to the greater retention of a molecular network by the higher molecular weight polymer, leading to more effective orientation with deformation.

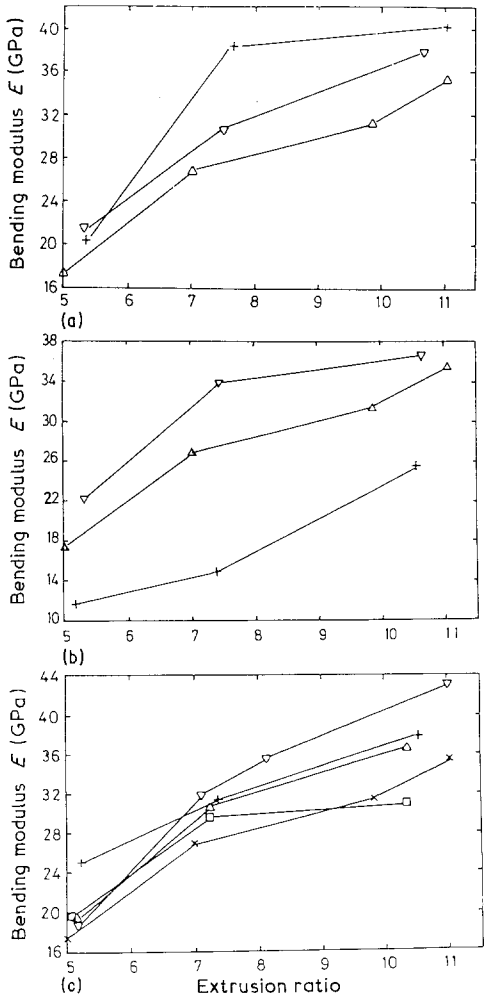

Figure 9 Bending modulus – extrusion ratio relationship for R006-60 extrudates pressure annealed with a variation from standard conditions (234° C for 1 h at 450 MPa). The effect is shown of variations in (a) temperature, (b) pressure and (c) time. (a) + 239° C, ▽ 237° C, △ 234° C, (b) △ 450 MPa, ▽ 475 MPa, + 500 MPa, (c) △ 10 mins, ▽ 15 mins, + 30 mins, × 60 mins, □ 180 mins.

3.5. Mechanical properties of extrudates

The bending modulus of the extrudates was determined from a standard three-point bend test and so gave a measure of the mechanical stiffness of the extrudates produced. The standard extrudate was considered to have been pressure annealed at 234° C for 1 h at 450 MPa pressure and Fig. 9 shows the effect of small variations of annealing temperature, time and pressure on the modulus of the extrudates.

Fig. 9a shows that a small increase in annealing pressure from the standard conditions produces an increase in bending modulus but when the pressure increases further and the annealing conditions become outside the intermediate phase, the modulus decreases significantly. Fig. 9b shows that the precise annealing temperature is also critical if optimum results are to be obtained. These results confirm the essential requirement, that pressure annealing must be carried out with a combination of pressure and temperature which establishes the polymer in the intermediate phase as defined by Bassett and Carder [3]. Fig. 9c shows the affect of annealing time on bending modulus and suggests that the very best results can be obtained for intermediate annealing times. This is presumably due to the conflicting requirements of producing an adequate degree of chain extension without producing a very high degree of molecular segregation, and also reducing chain entanglements to a very low level.

Fig. 10 compares the modulus-extrusion ratio relationships for extrudates of R006-60 polymer

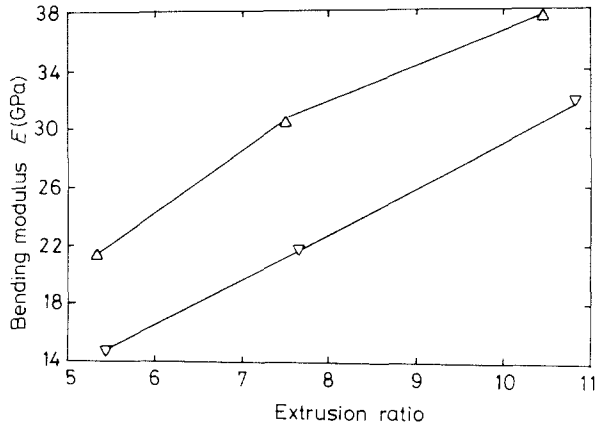

Figure 10 Bending modulus – extrusion ratio relationship for R006-60 extrudates pressure annealed and isothermally crystallized at high pressure (△ pressure annealed, ▽ isothermally crystallized at high pressure).

produced either by high pressure annealing or by high pressure crystallization from an initial molten state. It can be seen that, in spite of identical annealing conditions, the extrudates pressure crystallized from the molten polymer exhibit significantly lower moduli. However, the absolute values are still comparatively high and not in the very low range reported by Mead and Porter [5] for ram extrusion of low molecular weight polymer pressure crystallized in a similar manner. This difference emphasises again the primary requirement to retain the molecular network, with details of morphology and degree of chain extension playing important secondary roles.

3.6. Dynamic mechanical behaviour

Conventional melt-crystallized polyethylene and pressure annealed material have been hydrostatically extruded (extrusion ratio 10 : 1) and Fig. 11 shows the dynamic bending modulus E and the corresponding loss factor, tan δ of these extrudates. There are several differences to be noted. First, the bending modulus for the extrudate from pressure annealed material is significantly greater over the whole temperature range. This difference relates primarily to the reduction in the γ-relaxation process, presumably due to the increased crystallinity of the pressure-annealed material. Secondly, the temperature of the α-relaxation has increased from 30 to 60° C for the pressure-annealed extrudate compared with the conventional extrudate. This can be attributed to the very large increase in lamellar thickness and is consistent with the modelling by Hoffman *et al.* [6] of this process.

Fig. 12 provides an interesting insight into the effect of different annealing times on the mechanical properties of the extrudates. It can be seen that for the R006-60 grade polymer annealed at 234° C there is an optimum annealing time of 15 min to produce the highest values of bending and shear modulus. It will be shown later that these results are consistent with the view that these materials can be regarded as an aggregate of chain-extended units, and that on this basis there is a quantitative relationship between the bending and shear modulus for each type of specimen.

Fig. 13 provides a comparison of the dynamic bending modulus and shear modulus for two different grades of polymer R006-60 and H020-54P respectively,

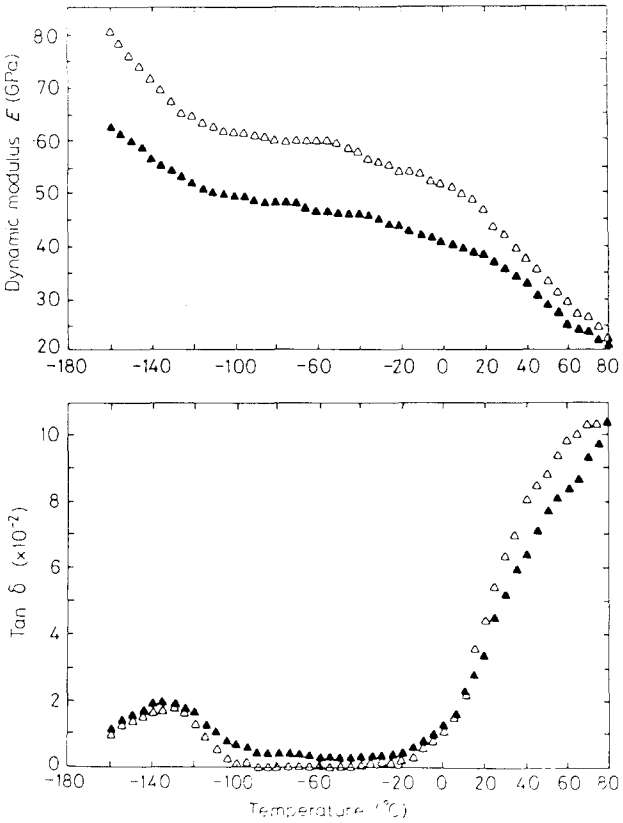

Figure 11 Dynamic three-point bend modulus (E) and mechanical loss factor (tan α) for R006-60 extrudates which have been initially either pressure annealed or isothermally crystallized at high pressure followed by hydrostatic extrusion. (Extrusion ratio 10 : 1), (△ pressure annealed, ▲ high pressure isothermally crystallized).

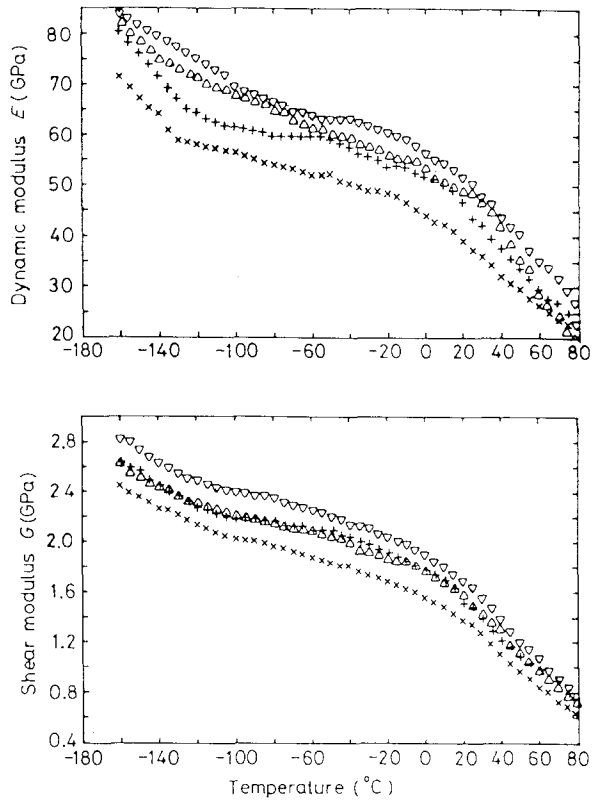

Figure 12 Dynamic modulus and shear modulus relationship with temperature of R006-60 extrudates which have been pressure annealed at 234° C and 450 MPa pressure for the time indicated and subsequently extruded. (Extrusion ratio 10 : 1). (△ 5 mins, ▽ 15 mins, + 1 h × 3 h).

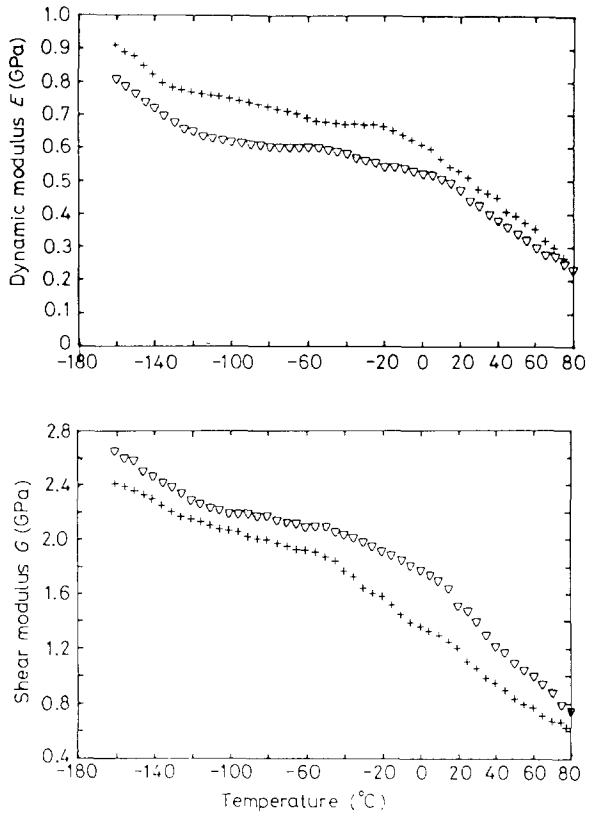

Figure 13 Dynamic modulus and shear modulus relationship with temperature of R006-60 and H020-54P extrudates which have been pressure annealed at 234° C for 1 h at 450 MPa pressure and subsequently extruded. (Extrusion ratio 10:1). (▽ R006-60, + H020-54P)

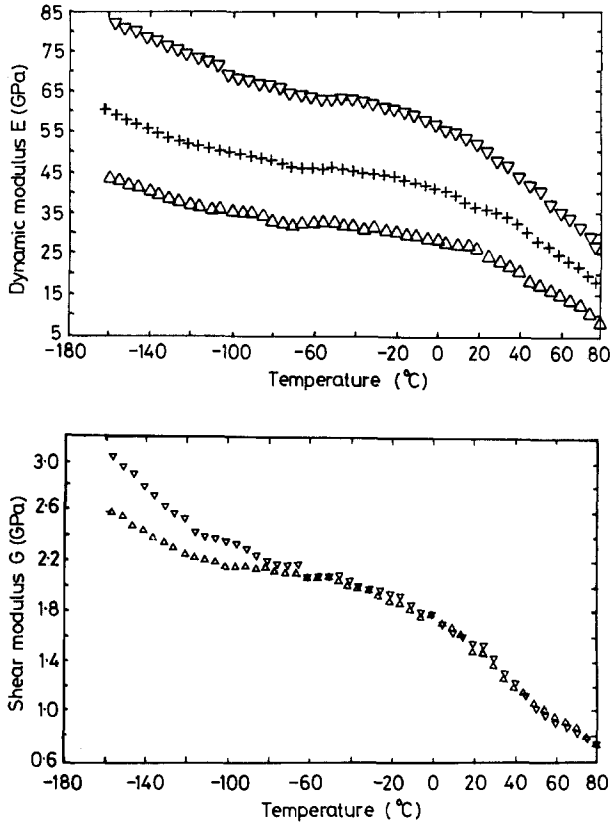

Figure 14 Dynamic modulus and shear modulus relationship with temperature of R006-60 extrudates which have been pressure annealed at 234° C for 1 h at 450 MPa pressure and subsequently extruded to the extrusion ratio indicated. (▽ 10:1, + 7:1, △ 5:1)

for identical pressure annealing treatments. It can be seen that whereas the bending modulus of the H020-54P grade is significantly higher than that for the R006-60 grade, the reverse situation applies for the shear moduli. This result will be discussed later, in terms of information gained from the aggregate model.

Finally, Fig. 14 shows the effect of extrusion ratio on the dynamic bending and shear behaviour. It can be seen that at all temperatures the bending stiffness increases very markedly with increasing extrusion ratio, consistent with the increase in molecular orientation. The shear modulus at high temperatures is not significantly affected by extrusion ratio. At low temperature, however, it is clearly reduced by increasing extrusion ratio. This result is consistent with the observations of Gibson *et al.* [7] for oriented polymers produced by hydrostatic extrusion of conventional bulk-crystallized polyethylene and explained quantitatively in terms of the aggregate model.

4. Discussion

Further insight on the anisotropic mechanical behaviour and on the increase in the extensional modulus with orientation during hydrostatic extrusion can be obtained by modelling the low strain mechanical properties in terms of the aggregate model [8].

The indications from the structural measurements presented in this paper, and from previous work, are that the deformation of chain-extended material during hydrostatic extrusion occurs without breakdown of this material. It is, therefore, very reasonable to consider that the specimen can be regarded as an aggregate of anisotropic units which are aligned by the solid phase deformation process. For simplicity it will be considered that the units are transversely isotropic and that their orientation is defined by the angle θ between the unique axis of the unit (assumed to be the chain axis i.e. the crystallographic c-axis direction) and the symmetry axis of the specimen, which is the extrusion direction.

The calculation of the elastic constants of the partially oriented polymer can be made either by averaging the compliance constants of the aggregate (the lower Reuss bound which assumes homogeneous stress) or by averaging the stiffness constants (the upper Voigt bound which assumes uniform strain). For the polymers investigated it has been shown that the lower Reuss bound is the more appropriate.

The extension compliance of the specimen in the extrusion direction S'_{33} is then given by

$$(S'_{33}) = S_{11}\langle\sin^4\theta\rangle + S_{33}\langle\cos^4\theta\rangle + (2S_{13} + S_{44})\langle\cos^2\theta\sin^2\theta\rangle \quad (1)$$

where $\langle\sin^4\theta\rangle$, $\langle\cos^4\theta\rangle$ and $\langle\sin^2\theta\cos^2\theta\rangle$ are the average values of $\sin^4\theta$ etc for the partially oriented polymer, and S_{11} and S_{33}, etc are the compliance constants of the anisotropic units.

If the polymer is highly oriented, as is the case of all the samples under consideration here,

$$\langle\cos^4\theta\rangle \sim 1, \langle\sin^4\theta\rangle \sim 0$$

and $\langle\cos^2\theta\sin^2\theta\rangle \sim \langle\sin^2\theta\rangle$

For polyethylene the shear compliance is also very large compared with the other compliances, so that we can neglect S_{13} in the last term of Equation 1.

With these simplifications we then have

$$(S'_{33}) = S_{33} + S_{44}\langle\sin^2\theta\rangle \quad (2)$$

It is important to note that although $\langle\sin^2\theta\rangle$ is small, because S_{44} is large compared with S_{33}, the second term in Equation 2 is comparable with the first in many instances. For the shear compliance of the specimen S'_{44} the aggregate model gives

$$\begin{aligned}\langle S'_{44}\rangle = {} & S_{11}(\langle 2\cos^2\theta\sin^2\theta\rangle + \langle\sin^2\theta\rangle) \\ & - S_{12}\langle\sin^2\theta\rangle - S_{13}\langle 4\cos^2\theta\sin^2\theta\rangle \\ & + S_{33}\langle 2\cos^2\theta\sin^2\theta\rangle + \tfrac{1}{2}S_{44}(\langle\sin^4\theta\rangle \\ & + \langle\cos^2\theta\rangle - \langle 2\cos^2\theta\sin^2\theta\rangle + \langle\cos^2\theta\rangle)\end{aligned} \quad (3)$$

Identical considerations to be adopted with regard to Equation 1 reduce Equation 2 to the very simple result

$$(S'_{44}) = S_{44} \quad (4)$$

The extensional compliance of the units S_{33} can be assumed to be the crystal chain modulus of polyethylene E_c, for which there are several estimates in the literature. For example, X-ray diffraction crystal strain measurements give a value of about 250 GPa [9]. Writing E as the tensile modulus of the sample and G as the shear modulus, Equations 2 and 4 can be combined to give

$$\frac{1}{E} = \frac{1}{E_c} + \frac{1}{G}\langle\sin^2\theta\rangle \quad (5)$$

Fig. 15 shows a plot of $1/E$ against $1/G$ for a range of R006-60 extrudates of different extrusion ratio, prepared from identical billets which have all been initially pressure annealed at 234° C for 15 min at 450 MPa pressure. The data certainly conform to the general relationship of the form proposed by Equation 5, individual points representing values of dynamic bending and shear modulus over the temperature range −160 to +80° C. The comparison between E and G can be taken one step further by comparing values of $\langle\sin^2\theta_c\rangle$ obtained on the basis of Equation 5 with X-ray diffraction results. These results are shown in Table III from which it appears that the X-ray diffraction results suggest rather lower orientation than the aggregate model, although the overall trend is similar in both cases. A possible explanation is that the domains of extended chain molecules are somewhat disordered, possibly due to the presence of segregated material. Indeed the comparison between values of $\langle P_2(\cos\theta_c)\rangle$ from both sources suggest a constant disorder within the "crystallites" of the aggregate model corresponding to $P_2(\cos 6°)$.

TABLE III Comparison of the values of $\langle\sin^2\theta_c\rangle$ obtained from X-ray diffraction measurements and from the aggregate model using R006-60 extrudates which have been initially pressure annealed at 234° C for 15 min at 450 MPa pressure

Extrusion ratio	$\langle\sin^2\theta_c\rangle$ X-ray diffraction	$\langle\sin^2\theta_c\rangle$ Aggregate model
5:1	0.095	0.059
7:1	0.048	0.039
10:1	0.036	0.026

Fig. 16 provides an interesting insight into the effect of differing annealing times on the mechanical properties of the extrudates. In this figure results for R006-60 polymer corresponding to four different annealing times ranging from 5 to 180 min are compared and all the results can be seen to lie on the same line. It can be concluded that $\langle\sin^2\theta_c\rangle$ as indicated by the X-ray diffraction measurements reported above, is independent of initial annealing time and that differences in tensile modulus relate to differences in the shear modulus of the materials. The indications from structural studies involving DSC measurements and SAXS are that the different annealing treatments may possibly change the segregation effects and so affect the shear modulus.

Fig. 17 provides a comparison of the values of $1/E$ and $1/G$ for the two grades of polyethylene under investigation. Although the results conform to Equation 5, there is a significantly lower value of $\langle\sin^2\theta_c\rangle$ for the H020-54P grade than for R006-60. This result is consistent with the X-ray diffraction data reported above. Although the bending moduli of the H020-54P extrudates are significantly higher than those for R006-60 material, the results previously discussed show the reverse to be true for the shear moduli. It is interesting that these results are all internally consistent in terms of the aggregate model.

Finally, there is a clear systematic curvature in the

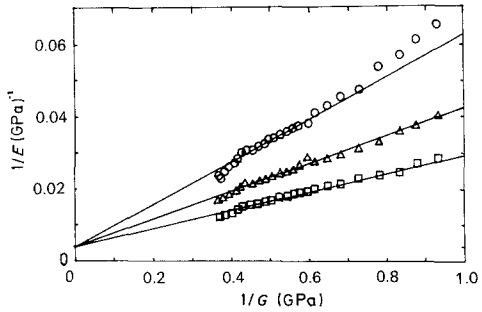

Figure 15 A plot of $1/E$ against $1/G$ showing the validity of the aggregate model analysis for a range of R006-60 extrudates previously pressure annealed at 234° C for 15 min at 450 MPa pressure. (□ 10:1, △ 7:1, ○ 5:1)

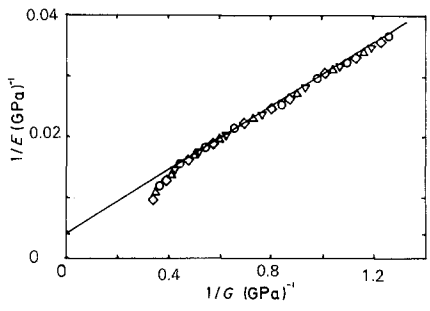

Figure 16 A plot of the aggregate model parameters for R006-60 extrudates (extrusion ratio 10:1) previously pressure annealed at 234° C at 450 MPa pressure for the time indicated. (△ 5 min, ◇ 15 min, ○ 60 min, ▽ 180 min)

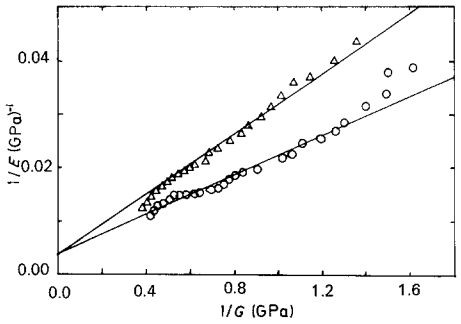

Figure 17 A plot of the aggregate model parameters for R006-60 and H020-54P extrudates (extrusion ratio 10 : 1), previously pressure annealed at 234° C for 15 min at 450 MPa pressure.

plots of $1/E$ against $1/G$ shown in Figs 15 and 17 which is also present in the 5 min annealing time results of Fig. 16 at higher values of $1/G$ than shown in the figure. It is likely that the discrepancies observed for data at high temperatures and low temperatures originate for different reasons. The origin of the curvature at low temperatures may be partly due to differences in the frequency of the bending and shear tests and this will be most important in the region of the γ relaxation process. Furthermore, the assumption that the observed shear modulus is identical to that of the hypothetical completely ordered aggregate unit may not hold in this region. It was shown that the shear modulus was sensitive to structure at low temperatures in the studies of Gibson *et al.* [7]. The curvature at high temperatures, is only evident in two cases, where the R006-60 and H020-54P billets were annealed for 5 min. It may well be that this annealing time gives rise to a less perfect chain-extended structure than when annealing for a longer time.

References

1. J. B. SAHARI, B. PARSONS and I. M. WARD, *J. Mater. Sci.* **20** (1985) 346–354.
2. H. H. CHUAH and R. S. PORTER, *J. Polym. Sci.* **22** (1984) 1353–1365.
3. D. C. BASSETT and D. R. CARDER, *Polymer* **14** (1973) 387.
4. D. C. BASSETT and B. TURNER, *Phil. Mag.* **29** (1974) 925.
5. W. T. MEAD and R. S. PORTER, *Int. J. Polym. Mater.* **1** (1979) 29.
6. J. D. HOFFMAN, G. WILLIAMS and E. A. PASSAGLIA, *J. Polym. Sci.* **C14** (1966) 173.
7. A. G. GIBSON, S. A. JAWAD, G. R. DAVIES and I. M. WARD, *Polymer* **23** (1982) 349.
8. I. M. WARD, *Proc. Phys. Soc.* **80** (1962) 1176.
9. J. CLEMENTS, R. JAKEWAYS and I. M. WARD, *Polymer* **19** (1978) 639.

Received 25 January
and accepted 13 February 1989